

Solvent-free Mechanochemistry of Two Thermochromic Schiff Bases

Branko Kaitner* and Marija Zbačnik

Faculty of Science, University of Zagreb, Department of Chemistry, Laboratory of General and Inorganic Chemistry, Horvatovac 102a, HR-10002 Zagreb, Croatia

* Corresponding author: E-mail: kaitner@chem.pmf.hr;
Phone: +385 1 4606 361; Fax: +385 1 4606 341

Received: 24-02-2012

Abstract

Two thermochromic Schiff bases mostly in keto-amine tautomeric form were obtained by means of mechanochemical synthesis. Both Schiff bases Compound **1** and Compound **2**, respectively are derived from the same primary amine 2-amino-5-methylphenol. Salicylaldehyde was used as aldehyde component in preparation of **1**, and *o*-vanillin as substituted salicylaldehyde component in synthesis of **2**. Powder products of the neat grinding and liquid-assisted grinding syntheses of **1** and **2** were compared with the crystalline products, obtained by recrystallization from a small amount of solvent. Both raw powder and recrystallized products were characterized and compared by means of PXRD, DSC and IR.

Keywords: Solvent-free mechanochemistry, Schiff bases, keto-enol tautomerism, thermochromism, crystal structure

1. Introduction

There is a permanent interest in the chemistry of the Schiff bases ever since Hugo Schiff reported their synthesis for the first time.^{1–4} During the past several decades Schiff bases are known as one of the most versatile in coordination chemistry.^{5,6} The particular interest is in their biological and pharmaceutical activities^{7–10} as well as in their photo- and thermochromic properties combined with the study of the keto-enol tautomerism *via* intramolecular proton transfer in solution and in the solid state.^{11–19} The thermochromism is defined as a reversible colour change caused by a temperature change.²⁰ In the period from 1962 to 1964 it was concluded that (i) the presence of the *ortho*-hydroxy group is of exceptional importance as it is included in the intramolecular hydrogen bond and facilitates the keto-enol tautomerisation *via* proton transfer and (ii) thermochromism occurs more often in planar (up to 25°) Schiff bases as a consequence of a change of electron density of imino nitrogen atom by temperature change.^{11–14} The first evidence of keto-enol equilibrium in the solid state was given in 1998.¹⁵ It was reported in 2007 that in the case of thermochromic Schiff bases the keto-enol tautomerism is not an exclusive reason for a colour

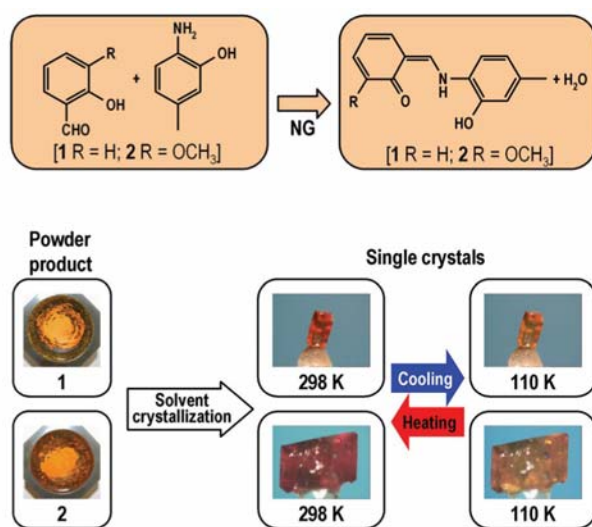
change. In that case fluorescence plays a crucial role in the solid state thermochromism at temperatures below room temperature.¹⁶

Much of interest on the other hand had been devoted to the investigation of the possibilities of designing new (almost) solvent-free techniques for the synthesis of (in)organic materials.²¹ The synthesis of Schiff bases and their coordination compounds *via* mechanochemical routes has the attention for some time.^{22–24} The importance of using the mechanochemical synthetic routes instead of conventional ones lies in avoiding large quantities of solvents and high temperatures and as it also sometimes gives products that are different from ones obtained from other synthetic methods.^{25–29} Schiff bases are conventionally synthesized including significant amounts of solvents and often at high temperatures.^{30–38} On the other hand neat grinding (NG) and liquid-assisted grinding (LAG) are encouraging because they are simple synthetic methods and beside being fast and environmentally more acceptable they are also successful.

Herein, we report the solvent-free synthesis (Scheme 1) of two Schiff bases derived from 2-amino-5-methylphenol (**2a5mp**) and salicylaldehyde (**sal**), Compound **1**, 6-[(2-hydroxy-4-methyl-phenylamino)-methylene]-cyclohexa-2,4-dienone, and *o*-vanillin (**ovan**), Com-

pound **2**, 6-[(2-hydroxy-4-methyl-phenylamino)-methylene]-2-methoxy-cyclohexa-2,4-dienone. Synthesis in solution, physico-chemical and spectroscopic characterization of Compound **1** were originally published in 2001³⁴ while the structural characterization of Compound **1** at room temperature was published in 2007 as a part of investigation on N–H...O induced structural changes on ketoenamines.³⁸

In this work we were concentrated on the search of the possible structural reasons of the thermochromic properties of these two compounds. Compounds **1** and **2** show thermochromic properties and are mostly in keto-amine tautomeric form at room and at low temperatures. Much of effort was devoted to the comparison of the powder products obtained by grinding and corresponding re-crystallized material.



Scheme 1. Mechanochemical neat grinding (NG) reaction. Lewis structure of more abundant keto-amine tautomeric form is pictured (top). Powder product of Compound **1** and **2**, respectively were crystallized from the solvent(s). Single crystals show distinctive colours at 298 K and 110 K (bottom).

2. Results and Discussion

2. 1. CSD Search

The main purpose of the CSD³⁹ search was to find out how many reported Schiff bases derived from **sal** and **ovan** are in keto-amine tautomeric form in the solid state. A search of the May 2012 release of CSD was made with the filtering criteria of a structural motif of a Schiff base with no halogen, carboxy acid, nitro, cyanide, PPh₂, NMe₂ or NEt₂ substituents on the amine moiety. The entries had to have their 3-D coordinates determined and exhibit no errors.

The search revealed that there are 34 entries of which 26 are reported as enol-imine, 7 as keto-amine tau-

tomers and 1 (NEDMUF) as “zwitter-ion” even though in the corresponding CIF file the H atom is bonded to N atom. We analyzed the bond distances for all of 34 entries. Taking into account the standard values of C-to-O and C-to-N single and double bond lengths in *ortho*-OH Schiff bases the POFWOX, NEDMUF, ZEXPEX, ZEXPEX01 and ZEXPEX02 entries are in keto-amine tautomeric form although reported in the CSD as enol-imines.^{4,40} The parameters for ETEYUX01 show that it is a superposition of both tautomers. It should be pointed out that the later six enol-imine entries and the 7 former unambiguously reported keto-amines are derived from 2-aminophenol and its derivatives except ETEYUX01 which is derived from 4-aminophenol. As such, all of them possess an additional OH group in the amine moiety that takes part in H-bonding with the O atom in the chelate ring. This intermolecular O–H...O hydrogen bond is in all cases somewhat shorter (except ETEYUX01) than the intramolecular N–H...O hydrogen bond. Taking part in the supramolecular bonding the OH group of the amine moiety influences the properties of these Schiff bases in the solid state and could affect on the predomination of keto-amine form.

It is stated in CSD for WOLYAX (derived from salicylaldehyde and 2-amino-4-methylphenol) that it is photochromic and in the paper of M. Kabak *et al.*³² as follows: *From some thermochromic and photochromic Schiff base compounds, it was proposed that molecules exhibiting thermochromy are planar, while those exhibiting photochromy are non-planar. In agreement with the above conclusions, the title compound is photochromic (M. Kabak, unpublished results) and the molecule is not planar; moieties A[C(1)-C(7), O(1)] and B[N(1), C(8)-C(14), O(2)] [both planar with a maximum deviation of –0.031(1) Å] are inclined at an angle of 24.3(1)°.* Nevertheless, the compound is thermochromic (our results to be published) and the H-atom in intramolecular O...N hydrogen bond is in disorder at room temperature (RT) and low temperature (LT). The molecule is at both temperatures mostly in keto-amine form and the relative ratio of keto vs. enol form is 80:20 at RT and 70:30 at LT. Many other similar cases with an additional OH group are a part of our investigation in progress.

2. 2. Powder X-Ray Diffraction Measurements

The powder X-ray diffraction (PXRD) pattern of grinding product **1** shows no diffraction maxima originated from **2a5mp** (Fig. 1). The pattern is in good agreement with the calculated one thus the desired product can be successfully obtained by means of mechanochemical synthesis.

The diffraction maxima of **ovan** and **2a5mp** can be seen in the PXRD pattern of NG product of the synthesis of **2** (Fig. 2) even after 8 months and in LAG product synthesized in the mortar manually. However these maxi-

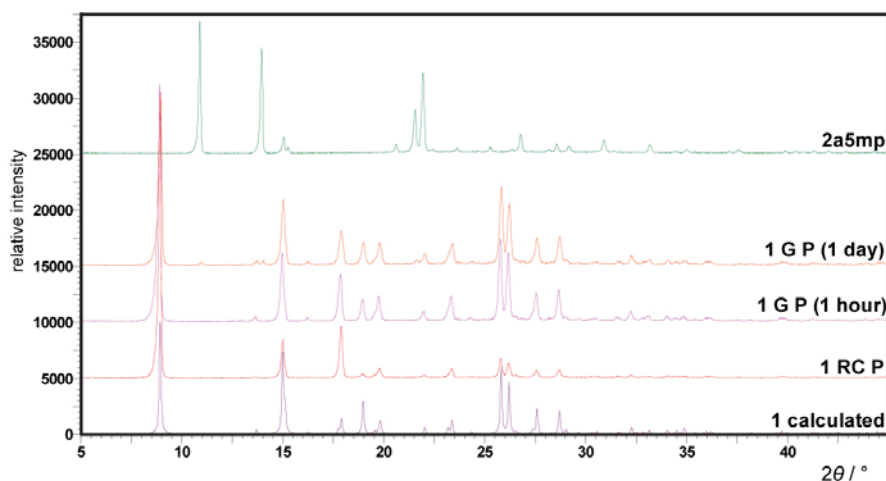


Figure 1. Calculated PXRD pattern of **1**, PXRD patterns of recrystallized product (1 RC P), grinding product after 1 hour (1 G P (1 hour)) and 1 day (1 G P (1 day)) and the pattern of **2a5mp**.

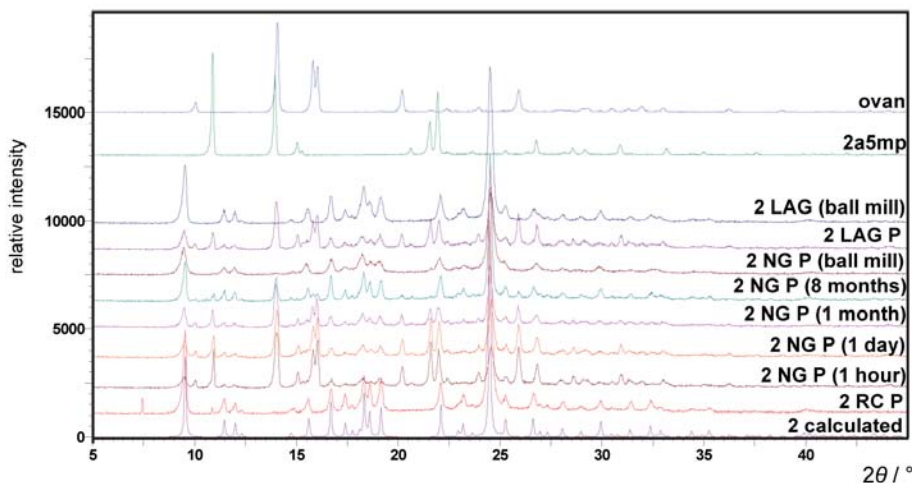


Figure 2. Calculated PXRD pattern of **2**, PXRD patterns of recrystallized product (2 RC P), manual NG product after 1 hour (2 NG P (1 hour)), 1 day (2 NG P (1 day)), 1 month (2 NG P (1 month)), 8 months (2 NG P (8 months)), ball mill NG product (2 NG P (ball mill)), manual LAG product, LAG ball mill product and the patterns of **2a5mp** and **ovan**.

ma are not present in the NG and LAG ball mill products. The diffraction maxima of the recrystallized material are in good agreement with the calculated pattern. It is evident that the synthesis by means of manual NG was successful but there are significant amounts of reactants in the product in case of **2**. Thus, the usage of LAG supplies the desired compound and the conversion of reactants into the product is complete.

2. 3. The Thermal Study

The DSC curve of grinding product **1** show one endothermic peak at 203 °C ($-51.8 \text{ kJ mol}^{-1}$) and recrystallized product also one endothermic peak at 201 °C ($-44.8 \text{ kJ mol}^{-1}$) which corresponds to the compound melting point. The synthesis in solution and physico-chemical and spectroscopic characteristics of Compound **1** were originally published in 2001.³⁴ Melting point was reported as

154–156 °C what differs significantly from our value. Due to this discrepancy we repeated the synthesis of **1** following precisely the synthetic procedure reported the synthetic procedure and determined the mp by DSC technique. The revealed value of 203 °C ($-41.6 \text{ kJ mol}^{-1}$) corresponded to our mp value. Because the mp differs in the case of different polymorph modifications we performed the PXRD experiment with crystals prepared as reported in the literature. The diffraction patterns showed to be identical in case of **1** whether the compound was synthesized in solution or by grinding procedure.

The DSC curve of manual NG product **2** show three endothermic peaks. The first peak at 45 °C (-5.0 kJ mol^{-1}) corresponds to the remains of **ovan** and the second peak at 156 °C (-0.6 kJ mol^{-1}) corresponds to **2a5mp**. The third endothermic peak at 218 °C ($-45.8 \text{ kJ mol}^{-1}$) corresponds to the Compound **2** melting point. The DSC curve of LAG product **2** show one endothermic peak at 219 °C

($-38.7 \text{ kJ mol}^{-1}$) that corresponds to the melting point of **2**. The DCS curve of recrystallized **2** show one endothermic peak at 218°C ($-45.8 \text{ kJ mol}^{-1}$), which corresponds to the compound melting point.

2. 4. Molecular and Crystal Structure

The aim of the work was to find out the possible structural reasons of the thermochromism of these two compounds at 298 K and 110 K, respectively through the results of single crystal X-ray structure analysis. Compound **1** and Compound **2** crystallize in monoclinic system with molecules in general position of the space groups $P2_1/c$ and $P2_1/n$, respectively. ORTEP-3 drawings of the molecules of Compound **1** and Compound **2** in keto-amine tautomeric form showing the crystallographic labelling scheme are shown in Figure 3.

compound of the same composition (Compound **1**) showed that it was isostructural with that one described in the literature. We performed a new X-ray structure determination of the same compound not to re-determine and re-refine already known and deposited crystal structure but to find out are there any stereochemical differences between molecular structure at RT and LT that could explain the thermochromism of Compound **1**.

The thermochromic phenomenon of Schiff bases depends in general on the keto-enol tautomer equilibrium in solid state. We directed our efforts to discover the keto-enol tautomer ratio of Compound **1** and **2** at RT and LT in three ways: (i) from the value of crucial bond lengths (O1–C2 and N1–C7) that define either keto-amine or enol-imine tautomer, (ii) from the position of hydrogen atom either in intramolecular N1–H...O1 or O1–H...N1 H-bond and (iii) from both (i) and (ii).

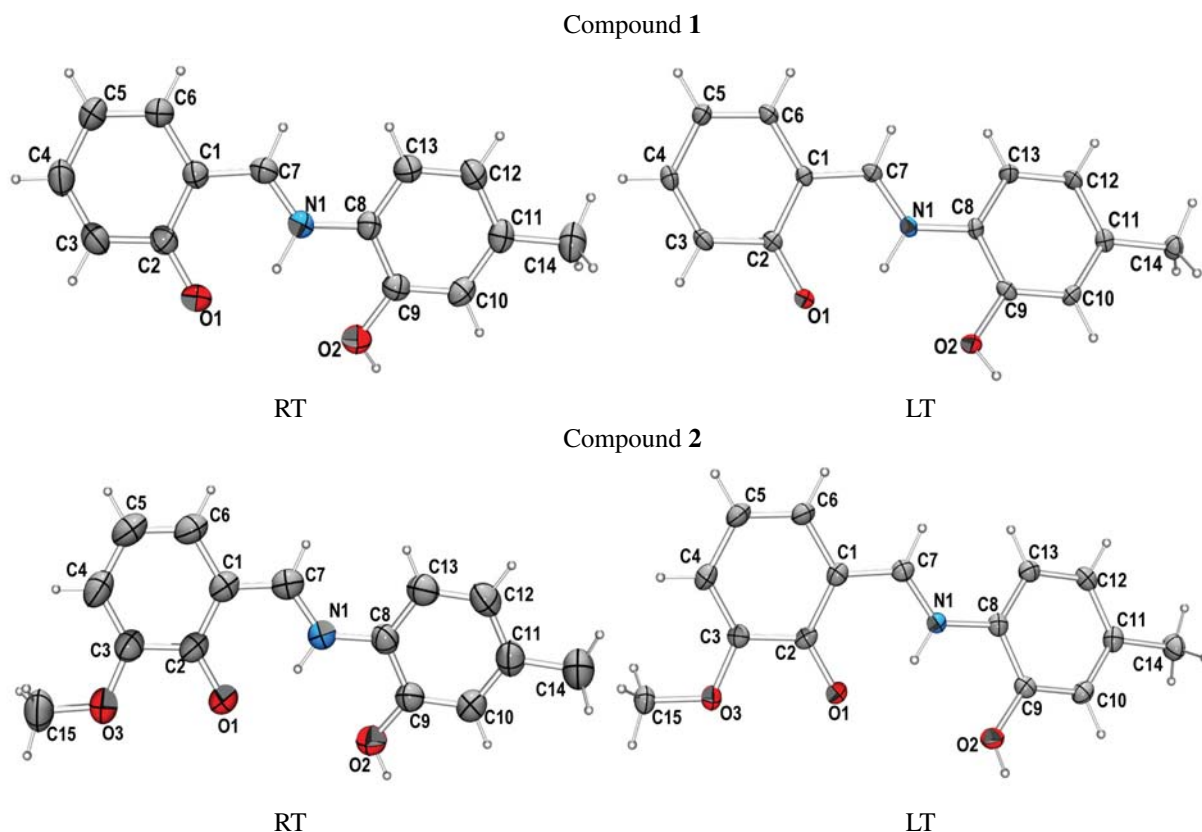


Figure 3. ORTEP-3⁴⁸ drawing of the keto-amine tautomer of Compound **1** and **2** at room temperature (RT) and at low temperature (LT) showing the crystallographic labelling scheme. Displacement ellipsoids are drawn at the 50 % probability level and H atoms are shown as small spheres of arbitrary radius.

The crystal structure of 6-[(2-hydroxy-4-methylphenylamino)-methylene]-cyclohexa-2,4-dienone based on the data collected at room temperature was solved in 2007 as a part of investigation of N–H...O induced structural changes on ketoenamines.³⁸ In that article the thermochromism of corresponding Schiff base was not commented in any sense. Our structure determination of the

(i) From the geometry parameters of **1** and **2** the type of the tautomer could not be discovered unequivocally. The O1–C2 and N1–C7 bond lengths correspond neither to single nor to double bond.⁴⁰ The later is *condicio sine qua non* either for keto-amine or enol-imine tautomer. The intermediate values of corresponding bond distances in **1** and **2** at RT and LT are listed in Table 1 follo-

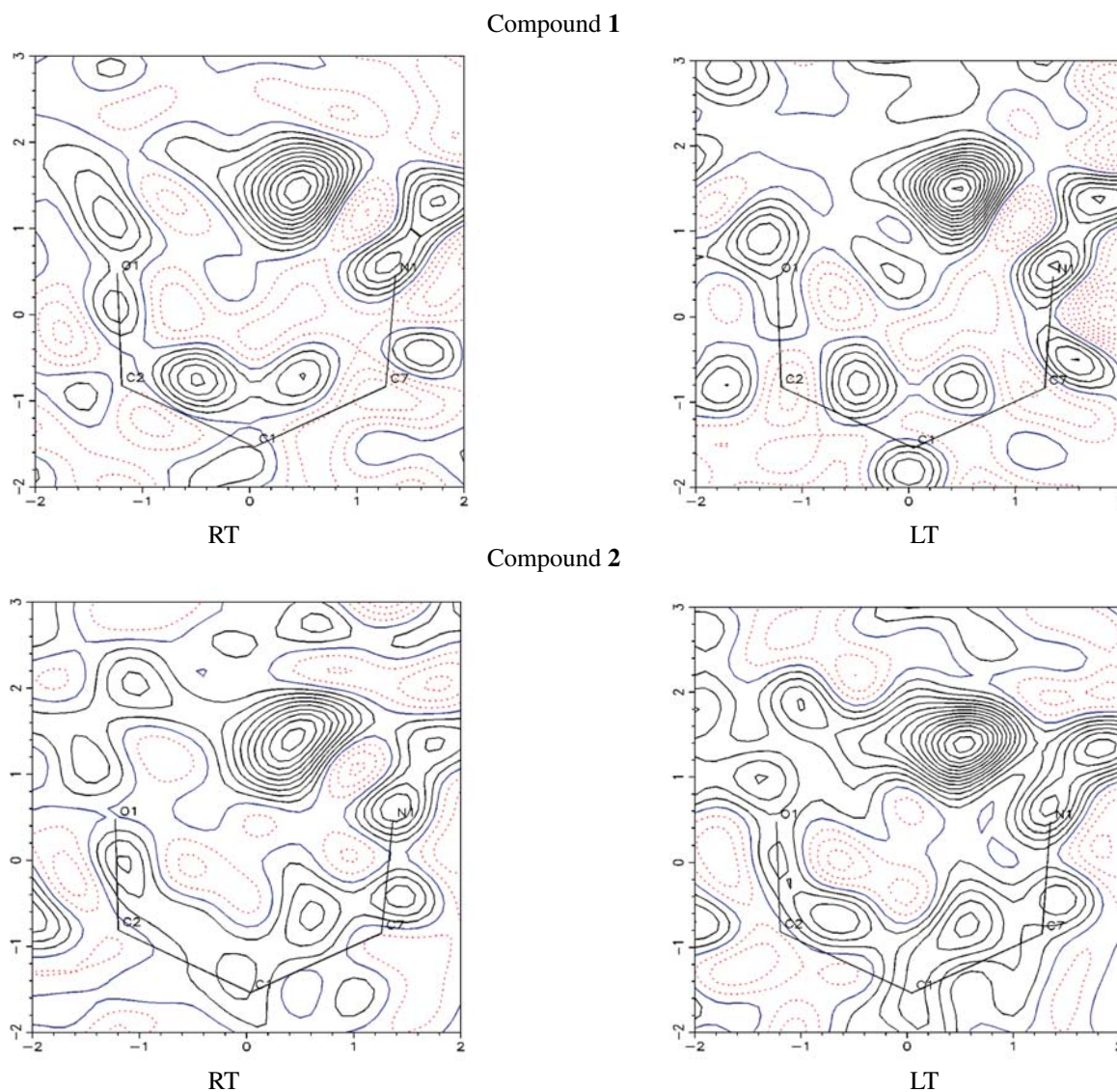
Table 1. Intermediate values of C2–O1 and C7–N1 bond distances in Compound **1** and **2** at RT and LT with corresponding generally accepted values of single and double bonds.⁴⁰

Compound 1				Compound 2			
RT		LT		RT		LT	
$d(\text{C2–O1})/\text{\AA}$	$d(\text{C7–N1})/\text{\AA}$	$d(\text{C2–O1})/\text{\AA}$	$d(\text{C7–N1})/\text{\AA}$	$d(\text{C2–O1})/\text{\AA}$	$d(\text{C7–N1})/\text{\AA}$	$d(\text{C2–O1})/\text{\AA}$	$d(\text{C7–N1})/\text{\AA}$
1.301(2)	1.293(2)	1.300(2)	1.301(2)	1.288(2)	1.309(2)	1.288(2)	1.308(2)
F. H. Allen <i>et al.</i> , <i>J. Chem. Soc. Perkin Trans. II</i> , 1987 , S1–S19.							
Keto-amine tautomer				Enol-imine tautomer			
$\text{C}=\text{C–NH–C}\# (\text{Nsp}^2 \text{ planar}) / \text{\AA}$		1.339		$\text{Car–C=N–C}\# / \text{\AA}$		1.279	
$\text{C=O (in benzoquinone)} / \text{\AA}$		1.230		$\text{Car–OH (in phenols)} / \text{\AA}$		1.362	

wing by the generally accepted ones.⁴⁰ From such data one can conclude only on superimposed tautomers at RT and LT and not on the tautomer ratio.

(ii) The hydrogen atom in chelate ring O1–C2–C1–C7–N1 showed in the δF map as a single, rather diffu-

se maximum located close to the N1 atom with minor broadening of electron density towards the O1 atom in both Compound **1** and **2** at RT as well as at the LT (Fig. 4). The shape and the position of peak representing the hydrogen atom(s) H1 in electron density maps indicate

**Figure 4.** Contour δF map calculated through N1–C7–C1–C2–O1 chelate ring of **1** and **2** at RT and LT with pronounced maximum representing the residual electron density corresponding to the position of H1 atom in intramolecular H-bond.

that both keto-amine and enol-imine tautomer are present in the crystal structure with predominate presence of keto-amine tautomer in both compounds at any of temperature.

Since the peak representing H1 atom appears in the δF map as quite diffuse, although single electron density maximum (Fig. 4) the tautomer ratio cannot be estimated from the results of X-ray structure determination. Nevertheless, the data on the peak level at RT and LT [Compound **1**: $0.495 e^-$ (RT); $0.560 e^-$ (LT); Compound **2**: $0.451 e^-$ (RT); $0.727 e^-$ (LT)] can be taken in consideration for the evaluation of the relative tautomer ratio at both temperatures. The residual electron density representing H1 atom in **1** and **2** is higher at 110 K. From these data a relative tautomer ratio can be calculated as follows:

Compound 1 :	$0.495 e^- : 0.560 e^- = 1 : 1.13$
Compound 2 :	$0.451 e^- : 0.727 e^- = 1 : 1.61$

From the ratios one can conclude that there exists 13% excess of keto-amine tautomer in Compound **1** at 110 K according to its presence at RT. Similarly, in Compound **2** there exists an excess of 61% of keto-amine tautomer at LT. Significantly higher presence of keto-amine tautomer in Compound **2** could be the result of different molecular interconnection in **2** (discrete dimers; Figure 5) vs. that one in **1** (infinite supramolecular chains³⁸). The 61% excess in Compound **2** at LT reflects in the separation of the residual electron density from N1 (0.92 \AA) in accordance with the same distance being 1.04 \AA at RT. The separation of the maximum apex representing the H1 atom in Compound **1** is the same at RT and LT amounting 1.01 \AA .

As salicylaldehyde derivatives both compounds possess a pseudo-aromatic chelate ring (N1–C7–C1–C2–O1) that contains a strong intramolecular N–H \cdots O hydrogen bond due to the short N \cdots O bite distance of $2.597(1) \text{ \AA}$ for **1** and $2.590(2) \text{ \AA}$ for **2** at RT, and $2.591(1) \text{ \AA}$ for **1** and $2.585(2) \text{ \AA}$ for **2** at LT. The shape of the molecules of **1** and **2** can be described *via* two terminal aromatic moieties linked by a N1–C7 bridge. Their stereochemistry is defined through mutual inclination of two terminal subunits, one being fused benzene, C1–to–C6 and pseudoaromatic chelate, N1–C7–C1–C2–O1 ring system and the other one being benzene, C8–to–C13 ring. There is a significant difference in interplanar angle between least-squares best planes calculated through the non-hydrogen atoms of terminal subunits in case of **1** and **2**, while the difference of the same dihedral angle at RT and LT in **1** and **2** is negligible [**1**: $14.93(5)^\circ$ (RT), $14.15(5)^\circ$ (LT); **2**: $20.84(6)^\circ$ (RT), $21.23(5)^\circ$ (LT)].

Present O and N hetero atoms, three in Compound **1** and four in Compound **2** affect the supramolecular interconnection through strong O–H \cdots O hydrogen bonds in both structures. Molecules of **1** produce infinite [010] chains through O2–H \cdots O1ⁱ H-bond equal to $2.574(2) \text{ \AA}$ (RT) and $2.559(2) \text{ \AA}$ (LT) [(i): $-x, y-1/2, -z+1/2$]. (For more details on molecular interconnection in **1** see Ref. 38).

More hetero atoms in **2** results in different supramolecular motif with crystal structure containing dimers as discrete units (Figure 5). The molecules dimerize through a strong O2–H \cdots O1ⁱⁱ H-bond of $2.590(2) \text{ \AA}$ (RT) and $2.584(1) \text{ \AA}$ (LT) [(ii): $-x, -y, -z$]. The intermolecular O2–H \cdots O1 bond is shorter than the intramolecular N1–H \cdots O1 bond in Compound **1** which is consistent with the ones reported for similar Schiff bases in keto-amine form. In Compound **2** they are the same. Bringing two molecules together by crystallographic inversion centre symmetry another weak interaction of type C10–H \cdots O3ⁱⁱ occurs at the distance of $3.334(2) \text{ \AA}$ (RT) and $3.289(2) \text{ \AA}$ (LT). Linking two molecules of **2** in discrete units can be described by hydrogen bond pattern set up by three rings. Corresponding graph set motif descriptors are $R_2^2(9)$ and $R_2^2(18)$, respectively.⁴¹ The dimers are involved in crystal packing through standard van der Waals interactions greater than 3.5 \AA .

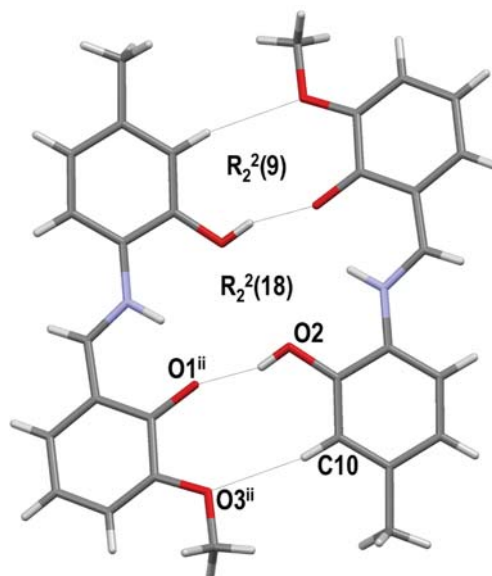


Figure 5. The dimers of **2** formed by two interactions, O2–H \cdots O1ⁱⁱ and C10–H \cdots O3ⁱⁱ through the symmetry operation of inversion centre.

Taking into consideration the values of bond lengths and bond angles as crucial geometry parameters for defining and comparing the similarity of molecular structures, the molecules of Compound **1** and Compound **2** are significantly the same at RT and LT according to 3σ criterion. Minor stereochemical difference appears only in the values of dihedral angles between terminal ring moieties as tri- in **1** and **2**.

3. Experimental

3.1. Preparations

Sal and ovan were purchased from Acros Organics, **2a5mp** from Merck, acetone and THF from Kemika, and

were used without further purification. All manual, neat grinding experiments were performed in an agate mortar. Equimolar quantities of **sal** (123 μL , 1 mmol) and **2a5mp** (0.123 g, 1 mmol) were ground for 30 minutes at 20 $^{\circ}\text{C}$ (Figure 6 (a)). For the first 20 minutes the reaction mixture is a liquid paste and afterwards the paste starts to solidify giving an orange powder (yield 98 %). Orange-red single crystals of **1** were obtained by slow evaporation from THF solution.

In case of all grinding experiments equimolar quantities of **ovan** (0.153 g, 1 mmol) and **2a5mp** (0.123 g, 1 mmol) were used. The reaction mixture was ground manually in agate mortar for 10 minutes at 20 $^{\circ}\text{C}$ (yield 99 %) (Figure 6 (b)). Ball mill experiments (NG and LAG) were performed in stainless steel jar of 10 mL volume using two stainless steel grinding balls, 7 mm in diameter (yield 99 % in both cases). LAG experiments were performed in the presence of 20 μL of acetone. A Retsch

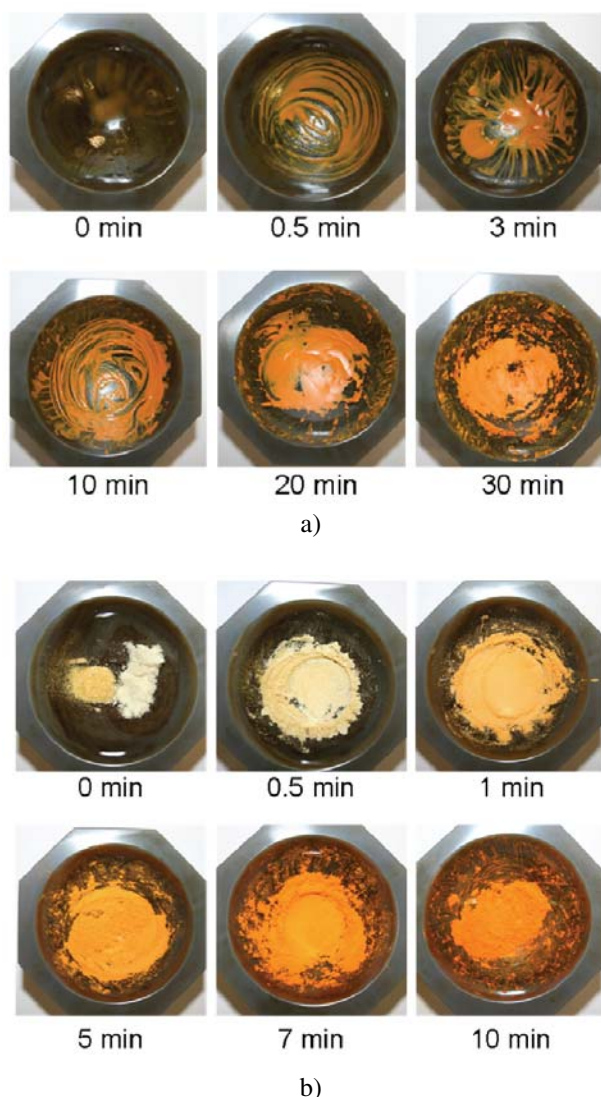


Figure 6. View of NG synthesis of (a) **1** and (b) **2** in an agate mortar.

MM200 grinder mill operating at 25 Hz frequency for 30 minutes was used for the synthesis. Red-pink single crystals of **2** were obtained by slow evaporation from acetone solution.

All reactions were doubled to ensure reproducibility. The successfulness was monitored by PXRD.

3. 2. Thermal and Spectroscopic Analysis

Thermal analysis was carried out on a Mettler Toledo DSC823 module in sealed aluminium pans (40 μL). Compound **1** and **2**, respectively were heated in flowing nitrogen atmosphere (200 mL min^{-1}) at a rate of 10 $^{\circ}\text{C min}^{-1}$. The data collection and spectral analysis were performed using the program package STARe Software 9.01.⁴²

Infrared spectra were recorded on an EQUINOX 55 FTIR spectrometer using a KBr pellet. The data collection and spectral analysis were performed using the program package OPUS 4.0.⁴³ In FT-IR spectra of **1** (grinding and recrystallized product) the weak broad band centered at 3453 cm^{-1} and 3441 cm^{-1} respectively can be assigned to the strong intramolecular N–H...O hydrogen bond. The spectra also show weak bands at 3045 cm^{-1} and at 2854 cm^{-1} that correspond to the aromatic C–H stretching vibration while those at 1596 cm^{-1} , 1531 cm^{-1} and 1504 cm^{-1} correspond to the aromatic C=C stretching. A strong band observed at 1633 cm^{-1} can be assigned to C–N stretching vibration. The band at 1290 cm^{-1} can be assigned to Car=O and that one at 1433 cm^{-1} to amino C–N stretching vibration.

In both, manual NG and recrystallized product FT-IR spectra of **2** weak broad band centered at 3425 cm^{-1} corresponds to strong intramolecular N–H...O hydrogen bond. The spectra also show weak bands at 2996 cm^{-1} , 2938 cm^{-1} (2923 cm^{-1} crystalline product) and at 2841 cm^{-1} (2849 cm^{-1} crystalline product) that correspond to the aromatic C–H stretching. The bands at 1600 cm^{-1} , 1540 cm^{-1} and at 1501 cm^{-1} correspond to the aromatic C=C stretching. A strong band observed at 1628 cm^{-1} (1626 cm^{-1} crystalline product) can be assigned to C–N stretching vibration. The band at 1300 cm^{-1} can be assigned to aromatic Car=O and that one at 1357 cm^{-1} to amino C–N stretching. The band at 1184 cm^{-1} can be assigned to Car–O–C.

NMR spectra were recorded on Varian Gemini XL 300 spectrometer. The spectral analysis was performed using the program package SpinWorks 3.⁴⁴ ^1H NMR of **2**: (300 MHz, DMSO) δ 14.13 (s, 1H, H1), 9.63 (s, 1H, H2), 8.92 (s, 1H, H7), 7.25 (d, J = 8.0 Hz, 1H, H13), 7.13 (dd, J = 7.8 Hz, 1H, H12), 7.03 (dd, J = 8.0 Hz, 1H, H4), 6.82 (t, J = 8.0 Hz, 1H, H5), 6.77 (s, 1H, H10), 6.69 (dd, J = 7.8 Hz, 1H, H6), 3.79 (s, 3H, Ar–O–CH₃), 2.23 (s, 3H, Ar–CH₃). ^{13}C NMR of **2**: (75 MHz, DMSO) δ 160.8 (C7), 152.3 (C9), 151.4 (C3), 148.6 (C2), 138.3 (C11), 132.3 (C8), 124.1 (C13), 120.8 (C12), 119.8 (C6), 119.6 (C5),

118.3 (C1), 117.5 (C4), 115.5 (C10), 56.3 (C15), 21.3 (C14).

3.3. X-Ray Structure Analysis

The molecular and crystal structures of **1** and **2** were determined by single crystal X-ray diffraction. The diffraction data were collected at 298 K and at 110 K (liquid nitrogen) for both compounds. Diffraction measurements were performed on an Oxford Diffraction Xcalibur Kappa CCD X-ray diffractometer using graphite-monochromator MoK_α radiation ($\lambda = 0.71073 \text{ \AA}$). The data sets were collected using the ω scans mode over the 2θ range up to 54° . Programs CrysAlis CCD and CrysAlis RED⁴⁵ were used for data collection, cell refinement and data reduction. The structures were solved by direct methods and refined using SHELXS and SHELXL programs, respectively.⁴⁶ The structural refinement was performed on F^2 using all data. The C-bound hydrogen atoms were placed in calculated positions and treated as riding on their parent atoms [$\text{C-H} = 0.93 \text{ \AA}$ and $U_{\text{iso}}(\text{H}) = 1.2 U_{\text{eq}}(\text{C})$]. The riding mode was dependent on type of hybridization





of C atom. The N-bound hydrogen atoms were located in the difference Fourier map and refined in subsequent refinement cycles. All calculations were performed using the WINGX crystallographic suite of programs.⁴⁷ The molecular structures of compounds are presented by ORTEP-3⁴⁸ and POV-RAY⁴⁹ programs. The hydrogen bonding projection was prepared using Mercury 2.3.⁵⁰ Table 2 comprises the general, X-ray diffraction and refinement data for both **1** and **2** at RT and LT.

PXRD experiments were performed on a PHILIPS PW 1840 X-ray diffractometer using CuK_α radiation ($\lambda = 1.54056 \text{ \AA}$) at 40 mA and 40 kV. The scattered intensities were measured with a scintillation counter. The angular range was from 3 to 45° (2θ) with steps of 0.02° , and the measuring rate was 1 s per step. The data collection and spectral analysis was performed using the program package Philips X'Pert.⁵¹

4. Conclusions

Two thermochromic Schiff bases mostly in keto-amine tautomeric form were obtained by means of mec-

Table 2. General, X-ray diffraction and refinement data for Compound **1** and **2**.

	Compound 1		Compound 2	
	RT	LT	RT	LT
Molecular formula	C ₁₄ H ₁₃ NO ₂		C ₁₅ H ₁₅ NO ₃	
<i>M</i> _r	227.25		257.28	
Crystal system	Monoclinic			
Space group	<i>P</i> 2 ₁ / <i>c</i>	<i>P</i> 2 ₁ / <i>n</i>		
<i>a</i> / Å	10.3265(9)	10.2065(6)	10.6222(9)	10.5493(9)
<i>b</i> / Å	9.3470(7)	9.3110(5)	11.3439(10)	11.2142(10)
<i>c</i> / Å	12.3201(12)	12.2427(8)	11.5162(11)	11.3375(10)
<i>β</i> / °	106.535(9)	107.003(6)	114.160(10)	113.791(10)
<i>V</i> / Å ³	1139.98(17)	1112.60(11)	1266.1(2)	1227.27(19)
<i>Z</i>	4		4	
<i>ρ</i> _{calc} / g cm ^{−3}	1.324	1.357	1.350	1.392
<i>λ</i> (Mo <i>K</i> _α) / Å, graphite monochromator	0.71073			
<i>T</i> / K	298	110	298	110
Crystal dimensions / mm ³	0.30 × 0.09 × 0.08		0.36 × 0.34 × 0.18	
Crystal colour and photography	orange-red	light orange	pink-red	orange
				
<i>μ</i> / mm ^{−1}	0.091	0.094	0.097	
<i>F</i> (000)	480		544	
<i>θ</i> range / °	4.49–27.00	4.55–27.00	4.27–26.99	4.28–27.00
Number of measured reflections	5211	4129	4524	4367
Number of independent reflections	2466	2410	2731	2653
Number of reflections with <i>I</i> ≥ 2σ(<i>I</i>)	1372	1496	1475	1973
Number of parameters	159		179	
Δ <i>ρ</i> _{max} , Δ <i>ρ</i> _{min} / e Å ^{−3}	0.139, −0.160	0.215, −0.241	0.171, −0.131	0.257, −0.218
<i>R</i> [<i>F</i> ² ≥ 2σ(<i>F</i> ²)]	0.0365	0.0390	0.0428	0.0430
<i>wR</i> (<i>F</i> ²)	0.0884	0.0921	0.1068	0.1147
Goodness-of-fit, <i>S</i>	0.841	0.888	0.828	0.963

hanochemical methods of synthesis. The PXRD patterns for **1** are in good agreement with the calculated one thus the desired product can be successfully obtained by means of mechanochemical synthesis. The synthesis of **2** by means of manual NG was successful but there are significant amounts of reactants in the product. Thus, the usage of LAG supplies the desired compound and the conversion of reactants into the product is complete. The molecular and crystal structures of **1** and **2** were solved by means of X-ray diffraction on single crystals at 298 K and at 110 K. When cooling, the crystal of **1** changes its colour from orange-red to light orange, and the crystal of **2** changes its colour from pink-red to orange. A relative tautomer ratio was calculated from the level of residual electron densities representing H1 atom in intramolecular hydrogen bond. The only conclusion that could be given is that there is a 13% excess of keto-amine tautomer in Compound **1** at 110 K according to its presence at RT. Similarly, in Compound **2** there exists an excess of 61% of keto-amine tautomer at LT. Significantly higher presence of keto-amine tautomer in Compound **2** could be the result of different molecular interconnection in **2**. The predomination of keto-amine tautomer in both cases is in correlation with intermolecular O–H...O hydrogen bonding. Molecules of **1** form infinite [010] chains and of **2** form dimers as solid state discrete units through the O–H...O hydrogen bonds.

The described results can have a great impact on the future aspects of green chemistry synthetic routes and are important for the understanding of keto-enol tautomerism and thermochromism of *o*-hydroxy Schiff base in the solid state.

5. Supplementary Material

Crystallographic data for the structural analysis have been deposited with the Cambridge Crystallographic Data Centre, CCDC No. 858694 and 858695 for Compound **1** at RT and LT and CCDC No. 858696 and 858697 for Compound **2** at RT and LT, respectively. Copies of these data may be obtained free of charge from the Director, CCDC, 12 Union Road, Cambridge, CB2 1EZ, UK (Fax: +44-1223-336033; email: deposit@ccdc.cam.ac.uk or www: <http://www.ccdc.cam.ac.uk>). FT-IR spectra, ¹H and ¹³C NMR spectra, DSC thermograms and PXRD patterns for all relevant materials are listed in Electronic Supporting Information.

6. Acknowledgements

This research was supported by the Ministry of Science, Education and Sport of the Republic of Croatia (Grant No. 119-1193079-3069).

7. References

1. H. Schiff, *Justus Liebigs Ann. Chem.*, **1864**, 131, 118–119.
2. U. Schiff, *Giornale di Scienze Naturali ed Economiche* Vol. II, Palermo, **1867**, 1–59.
3. T. T. Tidwell, *Angew. Chem., Int. Ed.*, **2008**, 47, 1016–1020.
4. A. Blagus, D. Cinčić, T. Friščić, B. Kaitner and V. Stilinović, *Maced. J. Chem. Int. Ed.*, **2010**, 29, 117–138.
5. M. Calligaris and L. Randaccio, *Comprehensive Coordination Chemistry*, ed. R. L. Reeves, **1985**, 2, 715–738 and references therein.
6. K. C. Gupta and A. K. Sutar, *Coord. Chem. Rev.*, **2008**, 252, 1420–1450.
7. H. K. Shapiro, *Am. J. Ther.*, **1998**, 5, 323–353.
8. H. Chen and J. Rhodes, *J. Mol. Med.*, **1996**, 74, 497–504.
9. H. Ünver, M. Yıldız, B. Dülger, Ö. Özgen, E. Kendi and T. N. Durlu, *J. Mol. Struct.*, **2005**, 737, 159–164.
10. B. Chattopadhyay, S. Basu, P. Chakraborty, C. K. Choudhuri and A. K. Mukherjee, *J. Mol. Struct.*, **2009**, 932, 90–96.
11. M. D. Cohen and G. M. J. Schmidt, *J. Phys. Chem.*, **1962**, 66, 2442–2445.
12. M. D. Cohen, G. M. J. Schmidt and S. Flavian, *J. Chem. Soc.*, **1964**, 2041–2051.
13. M. D. Cohen, Y. Hirshberg and G. M. J. Schmidt, *J. Chem. Soc.*, **1964**, 2051–2059.
14. E. Hadjoudis, M. Vitorakis and I. M. Mavridis, *Tetrahedron*, **1987**, 43, 1345–1360.
15. K. Ogawa, Y. Kasahara, Y. Ohtani and J. Harada, *J. Am. Chem. Soc.*, **1998**, 120, 7107–7108.
16. K. Ogawa and J. Harada, *J. Mol. Struct.*, **2003**, 647, 211–216.
17. E. Hadjoudis and I. M. Mavridis, *Chem. Soc. Rev.*, **2004**, 33, 579–588.
18. A. Ohshima, A. Momotake and T. Arai, *J. Photochem. Photobiol., A*, **2004**, 162, 473–479.
19. J. Harada, T. Fujiwara and K. Ogawa, *J. Am. Chem. Soc.*, **2007**, 129, 16216–16221.
20. H. Bouas-Laurent and H. Dürr, *Pure Appl. Chem.*, **2001**, 73, 639–665.
21. S. L. James, C. J. Adams, C. Bolm, D. Braga, P. Collier, T. Friščić, F. Grepioni, K. D. M. Harris, G. Hyett, W. Jones, A. Krebs, J. Mack, L. Maini, A. Guy Orpen, I. P. Parkin, W. C. Shearouse, J. W. Steed and D. C. Waddelli, *Chem. Soc. Rev.*, **2012**, 41, 413–447.
22. G. Rothenberg, A. P. Downie, C. L. Raston and J. L. Scott, *J. Am. Chem. Soc.*, **2001**, 123, 8701–8708.
23. O. Dolotko, J. W. Wiench, K. W. Dennis, V. K. Pecharsky and V. P. Balema, *New J. Chem.*, **2010**, 34, 25–28.
24. D. Cinčić and B. Kaitner, *CrystEngComm*, **2011**, 13, 4351–4357.
25. D. Braga and F. Grepioni, *Angew. Chem., Int. Ed.*, **2004**, 43, 4002–4011.
26. A. V. Trask, W. D. S. Motherwell and W. Jones, *Int. J. Pharm.*, **2006**, 320, 114–123.
27. A. Pichon and S. L. James, *CrystEngComm*, **2008**, 10, 1839–1847.

28. T. Friščić and W. Jones, *Faraday Discuss.*, **2007**, 136, 167–178.
29. D. Cinčić, T. Friščić and W. Jones, *J. Am. Chem. Soc.*, **2008**, 130, 7524–7525.
30. A. Elmali and Y. Elerman, *J. Mol. Struct.*, **1998**, 442, 31–37.
31. A. Elmali, Y. Elerman and C. T. Zeyrek, *J. Mol. Struct.*, **1998**, 443, 123–130.
32. M. Kabak, A. Elmali and Y. Elerman, *J. Mol. Struct.*, **1999**, 477, 151–158.
33. A. Elmali, M. Kabak and Y. Elerman, *J. Mol. Struct.*, **1999**, 484, 229–234.
34. V. Barba, D. Cuahutle, R. Santillan and N. Farfán, *Can. J. Chem.*, **2001**, 79, 1229–1237.
35. P. G. Lacroix, F. Averseng, I. Malfant and K. Nakatani, *Inorg. Chim. Acta*, **2004**, 357, 3825–3835.
36. V. T. Kasumov, Ş. Özal-Yaman and E. Taş, *Spectrochim. Acta, Part A*, **2005**, 62, 716–720.
37. R. Kannappan, D. M. Tooke, A. L. Spek and J. Reedijk, *Inorg. Chim. Acta*, **2006**, 359, 334–338.
38. M. Rodríguez, R. Santillan, Y. López, N. Farfán, V. Barba, K. Nakatani, E. V. García Baéz and I. I. Padilla-Martínez, *Supramol. Chem.*, **2007**, 19, 641–653.
39. F. H. Allen, *Acta Crystallogr.*, **2002**, B58, 380–388.
40. F. H. Allen, O. Kennard, D. G. Watson, L. A. Brammer and G. Orpen, *J. Chem. Soc. Perkin Trans. II*, **1987**, S1–S19.
41. J. Bernstein, R. E. Davis, L. Shimoni and N.-L. Chang, *Angew. Chem. Int. Ed. Engl.*, **1995**, 34, 1555–1573.
42. STARe Software V.9.01., Mettler Toledo GmbH, **2006**.
43. OPUS 4.0., Bruker Optik GmbH, **2003**.
44. K. Marat, SpinWorks 3, Version 3.1.0.0., **2009**, <http://home.cc.umanitoba.ca/~wolowiec/spinworks/index.html>
45. Oxford Diffraction, Oxford Diffraction Ltd., Xcalibur CCD system, CrysAlis CCD and CrysAlis RED software, Version 1.170, **2003**.
46. G. M. Sheldrick, *Acta Crystallogr., Sect A: Found. Crystallogr.*, **2008**, A64, 112–122.
47. L. J. Farrugia, WinGX, *J. Appl. Crystallogr.*, **1999**, 32, 837–838.
48. L. J. Farrugia, ORTEP-3 for Windows, *J. Appl. Crystallogr.*, **1997**, 30, 565–566.
49. Persistence of Vision Pty (**2004**) Persistence of Vision Ray-tracer (POV-RAY). Version 3.6. <http://www.povray.org/download/>.
50. C. F. Macrae, I. J. Bruno, J. A. Chisholm, P. R. Edgington, P. McCabe, E. Pidcock, L. Rodriguez-Monge, R. Taylor, J. v. d. Streek and P. A. Wood, *J. Appl. Crystallogr.*, **2008**, 41, 466–470.
51. Philips X'Pert Data Collector 1.3e, Philips Analytical B.V. Netherlands: Philips X'Pert Graphics & Identify 1.3e Philips Analytical B.V. Netherlands, **2001**.

Povzetek

Avtorji so s pomočjo mehanokemične sinteze pripravili dve termokromni Schiffovi bazi, ki se pretežno nahajata v keto-imin tautomerni obliki. Obe Schiffovi bazi, poimenovani kot spojina **1** in spojina **2**, sta bili pripravljene iz 2-amino-5-metilfenola. Za pripravo spojine **1** so kot aldehydno komponento uporabili salicilaldehid, za pripravo spojine **2** pa *o*-vanilin. Oba praškasta produkta dobljena pri sintezi s suhim mešanjem in trenjem, kot tudi pri enakem postopku ob sistenci topila, so primerjali s kristaliničnimi produkti, dobljenimi s prekristalizacijo iz majhne količine topila. Vsi produkti, tako praškasti kot tudi kristalinični, so bili okarakterizirani s PXRD, DSC in IR metodami.

Supporting information

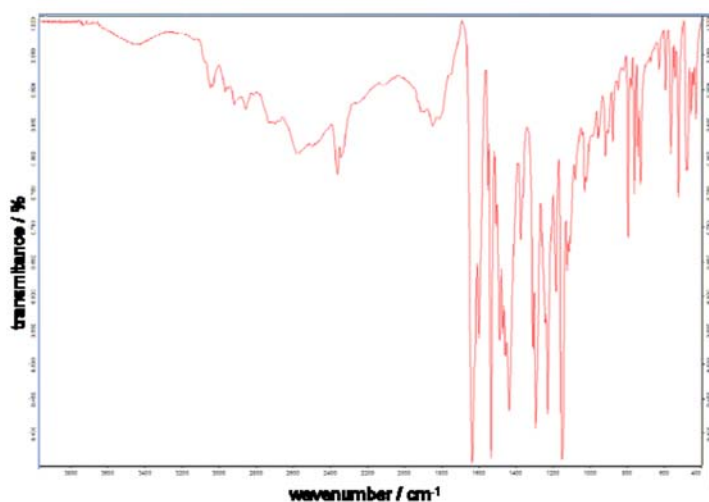


Figure S1. IR spectrum for compound 1 – grinding product 2

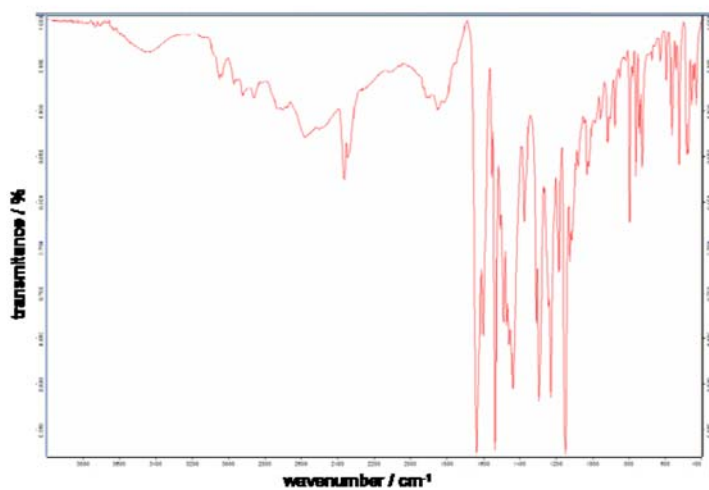


Figure S2. IR spectrum for compound 1 – recrystallized product 2

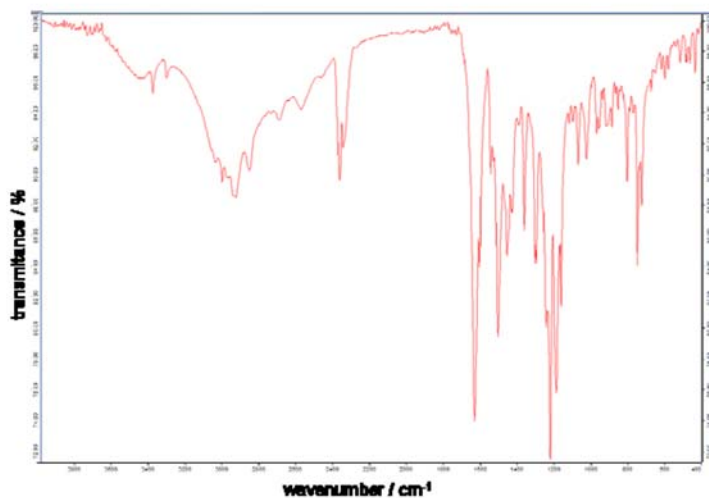


Figure S3. IR spectrum for compound 2 – grinding product 2

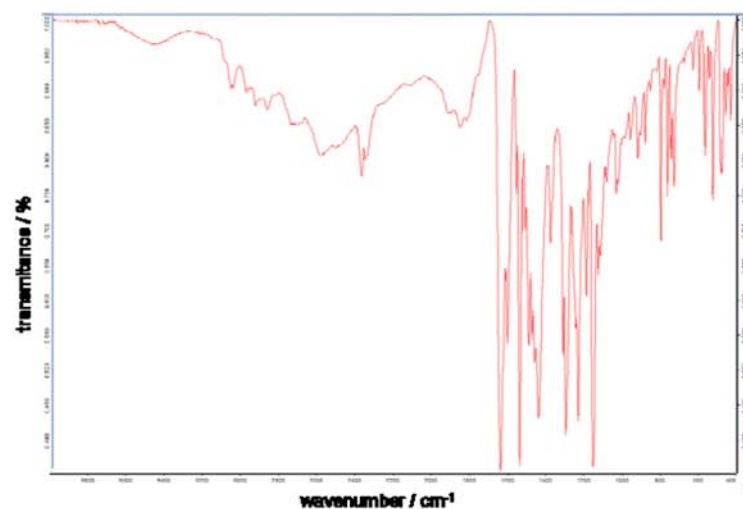


Figure S4. IR spectrum for compound **2** – recrystallized product **3**

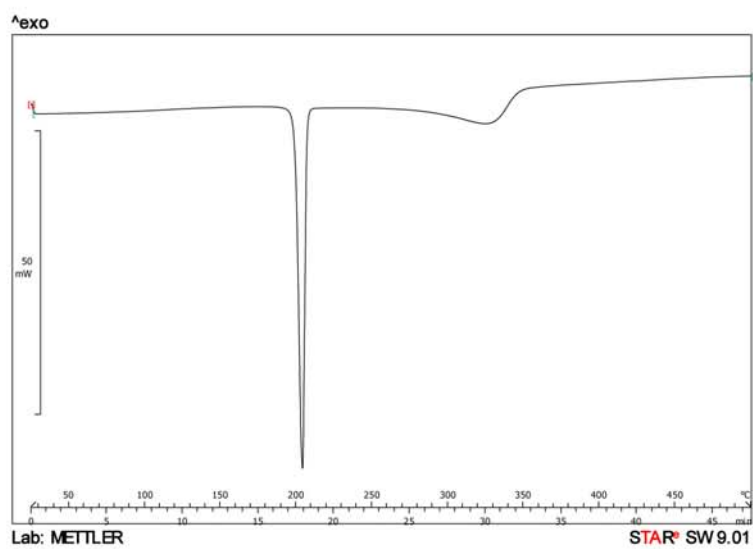


Figure S5. DSC curve for compound **1** – grinding product **3**

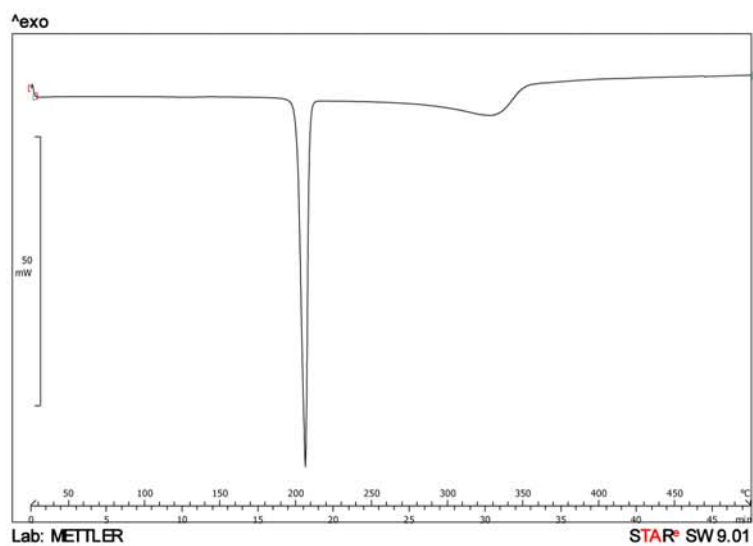


Figure S6. DSC curve for compound **1** – recrystallized product **3**

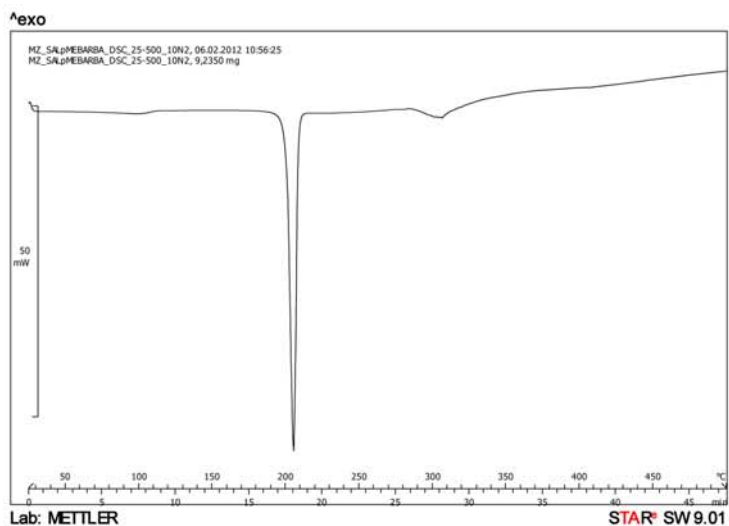


Figure S7. DSC curve for compound 1 – synthesized as reported by Barba *et al.* 4

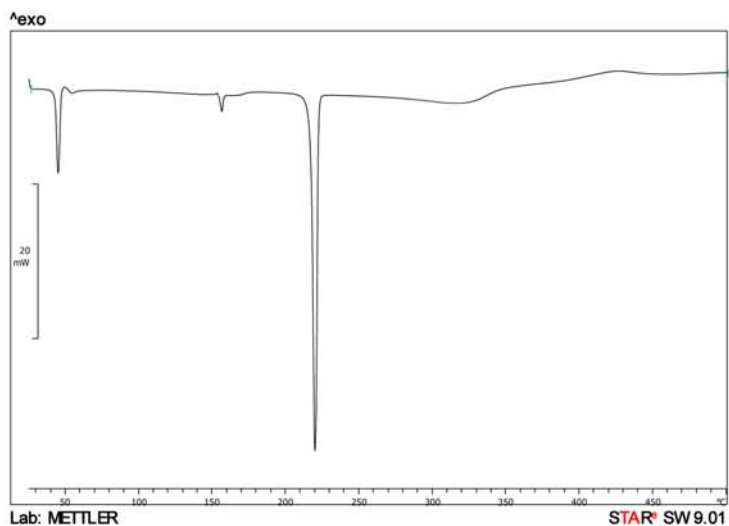


Figure S8. DSC curve for compound 2 – manual NG product 4

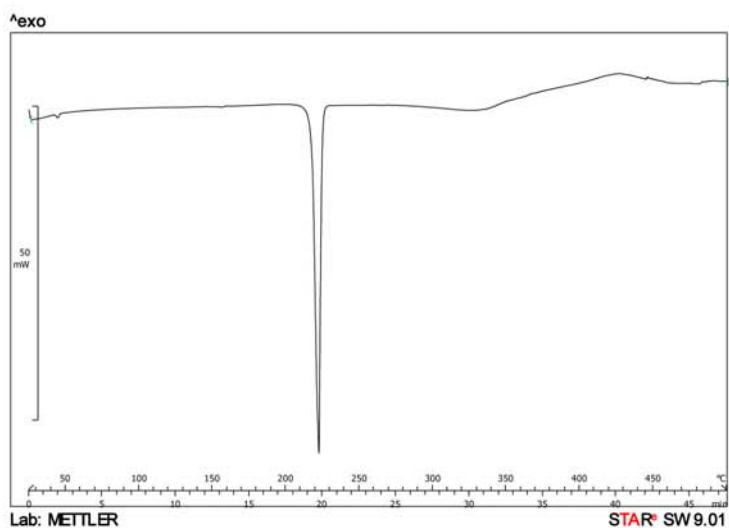


Figure S9. DSC curve for compound 2 – ball mill LAG product 4

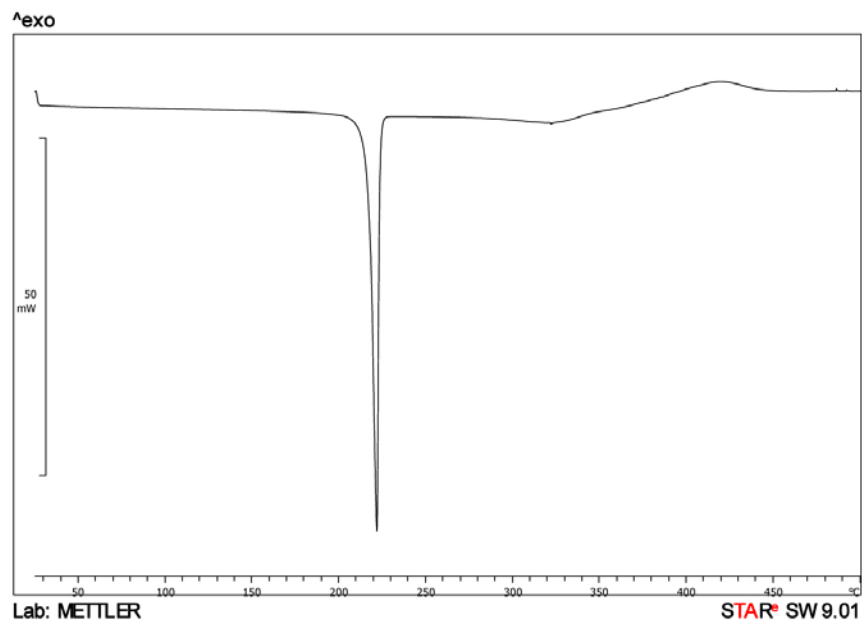


Figure S10. DSC curve for compound 2 – recrystallized product 5

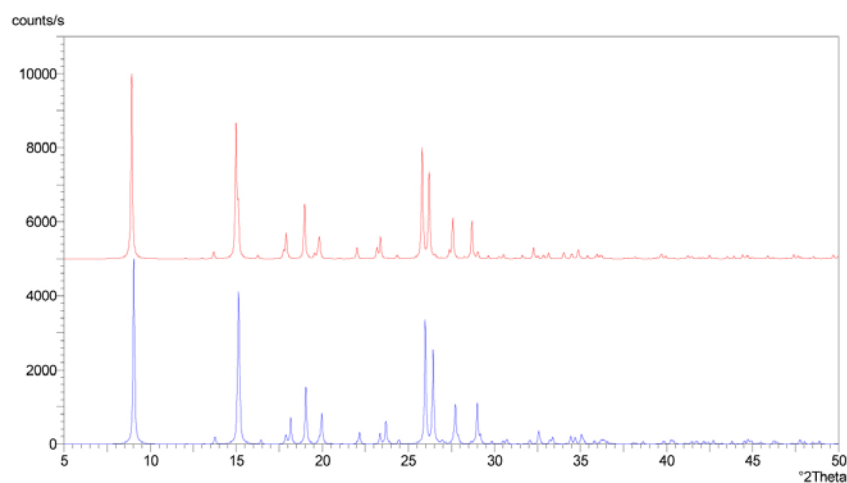


Figure S11. Calculated PXRD patterns for compound 1 at RT and at LT 5

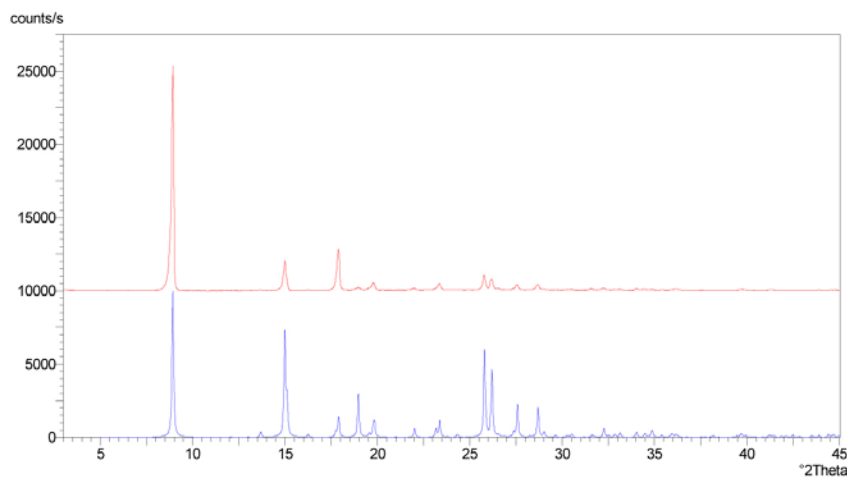


Figure S12. Calculated PXRD pattern for compound 1 at RT and the pattern of 5 recrystallized product

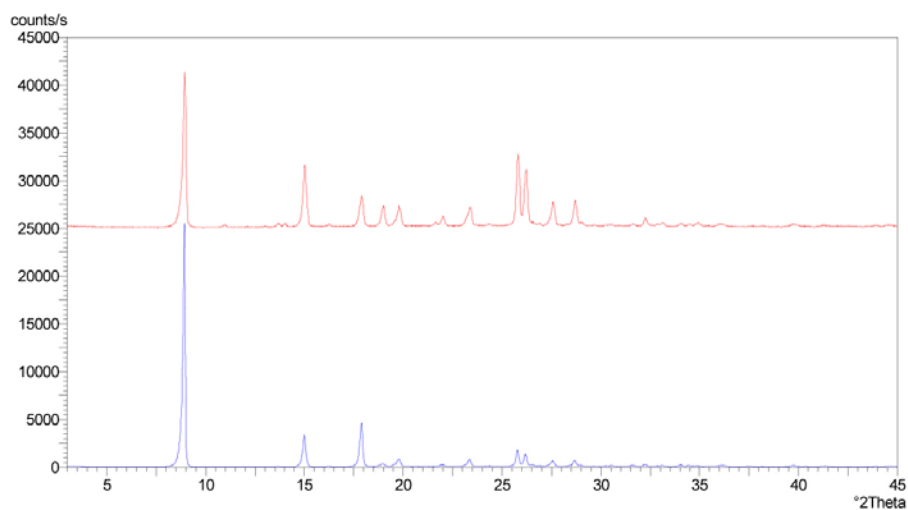


Figure S13. PXRD patterns for grinding product of the synthesis of **1** after 1 hour and 6 after 1 day

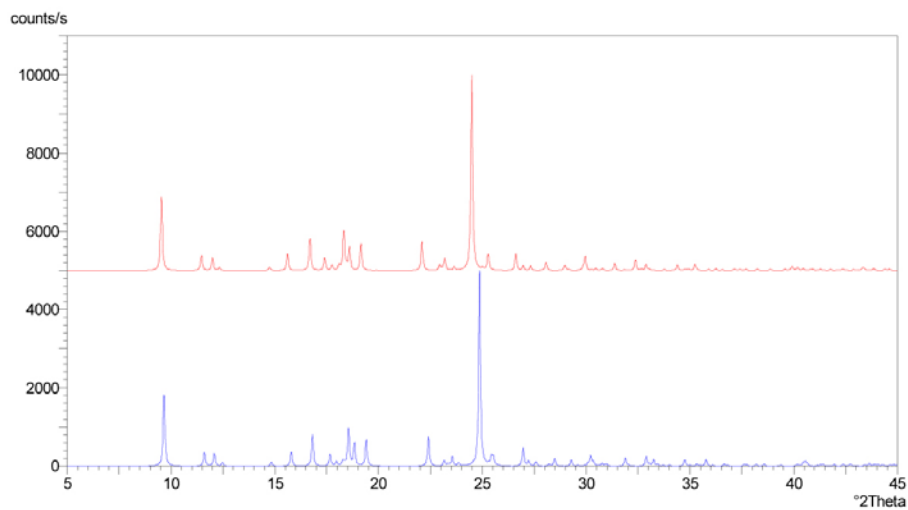


Figure S14. Calculated PXRD patterns for compound **2** at RT and at LT 6

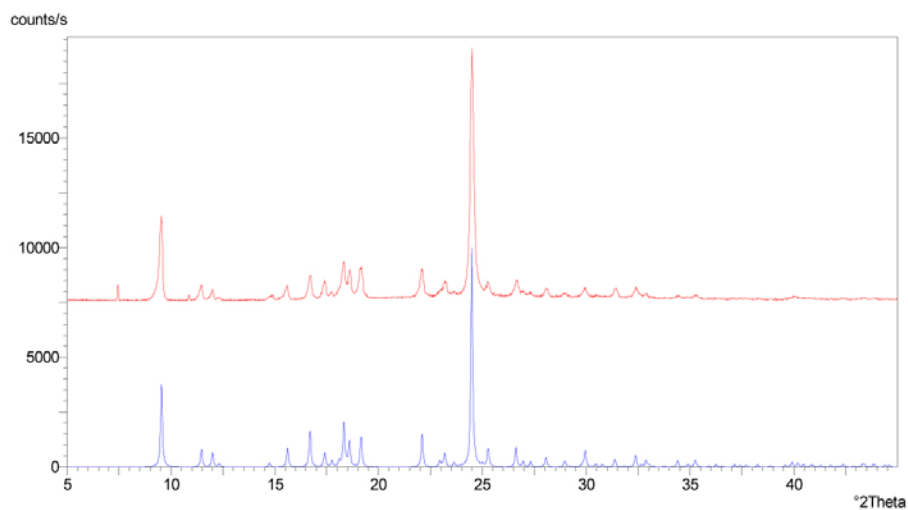


Figure S15. Calculated PXRD pattern for compound **2** at RT and the pattern of 6 recrystallized product

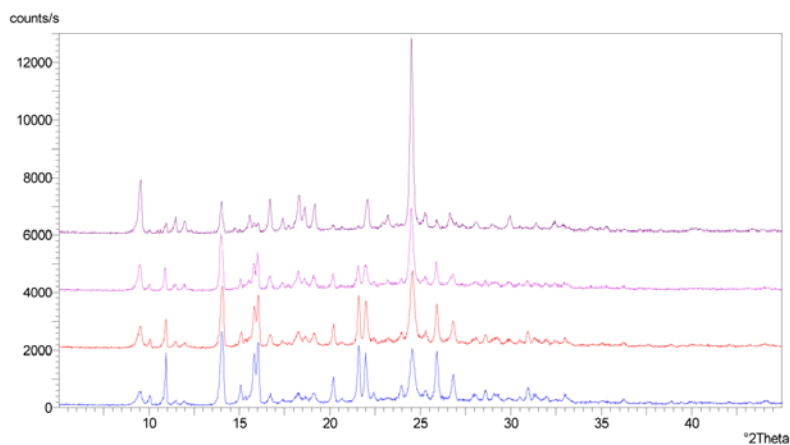


Figure S16. PXRD patterns for grinding product of the synthesis of **2** after 1 hour, 1 day, 7 1 month and 8 months

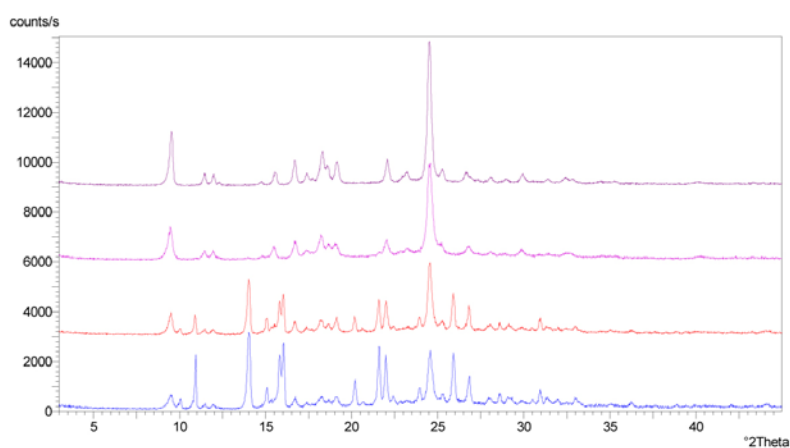


Figure S17. PXRD patterns for grinding product of the synthesis of **2** for the NG and 7 LAG syntheses in the agate mortar and in the ball mill

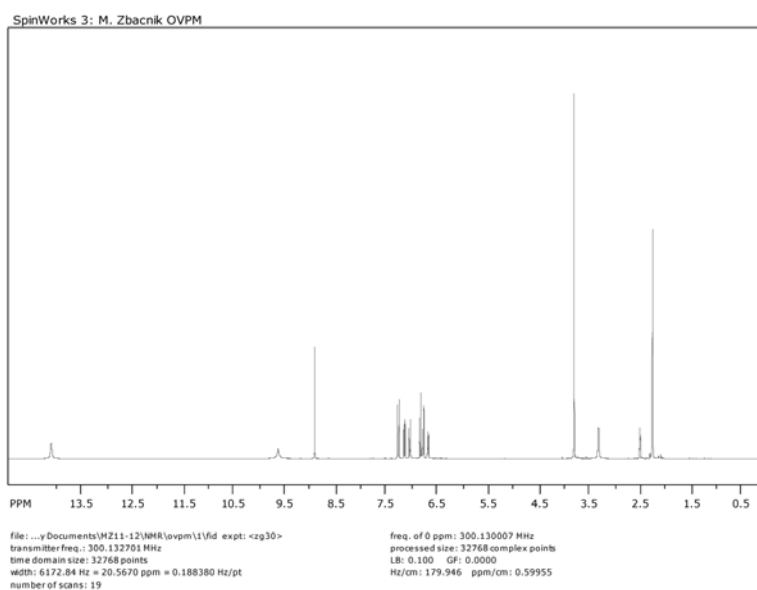


Figure S18. ¹H NMR spectra for compound **2**

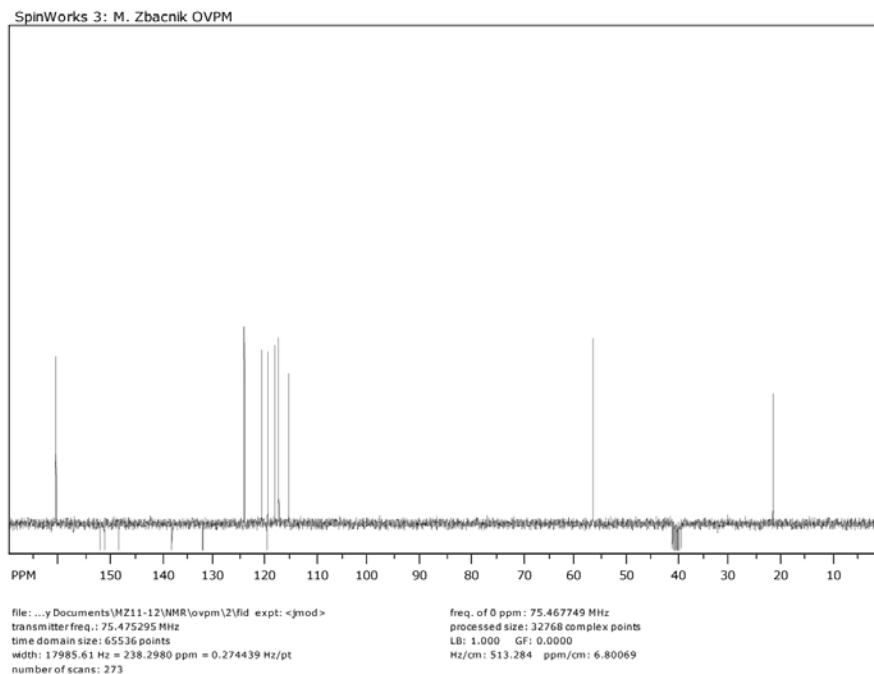


Figure S19. ^{13}C NMR spectra for compound **28**